

5-Aminolevulinic Acid-Squalene Nanoassemblies for Tumor Photodetection and Therapy: In Vitro Studies

BABIC, Andréj, *et al.*

Abstract

Protoporphyrin IX (PpIX) as natural photosensitizer derived from administration of 5-aminolevulinic acid (5-ALA) has found clinical use for photodiagnosis and photodynamic therapy of several cancers. However, broader use of 5-ALA in oncology is hampered by its charge and polarity that result in its reduced capacity for passing biological barriers and reaching the tumor tissue. Advanced drug delivery platforms are needed to improve the biodistribution of 5-ALA. Here, we report a new approach for the delivery of 5-ALA. Squalenoylation strategy was used to covalently conjugate 5-ALA to squalene, a natural precursor of cholesterol. 5-ALA-SQ nanoassemblies were formed by self-assembly in water. The nanoassemblies were monodisperse with average size of 70 nm, polydispersity index of 0.12, and ζ -potential of +36 mV. They showed good stability over several weeks. The drug loading of 5-ALA was very high at 26 %. In human prostate cancer cells PC3 and human glioblastoma cells U87MG PpIX production was monitored in vitro upon the incubation with nanoassemblies. The results showed that they were highly efficient in generating [...]

Reference

BABIC, Andréj, *et al.* 5-Aminolevulinic Acid-Squalene Nanoassemblies for Tumor Photodetection and Therapy: In Vitro Studies. *Nanoscale Research Letters*, 2018, vol. 13, no. 10

DOI : 10.1186/s11671-017-2408-y

PMID : 29327259

Available at:

<http://archive-ouverte.unige.ch/unige:103500>

Disclaimer: layout of this document may differ from the published version.



UNIVERSITÉ
DE GENÈVE

5-aminolevulinic acid-squalene nanoassemblies for tumor photodetection and therapy: *in vitro* study

Babič A.^{1,*}, Herceg V.¹, Bastien E.^{2,3}, Lassalle, H.-P.^{2,3}, Bezdetnaya, L.^{2,3}, and Lange N.^{1,*}

Abstract

Protoporphyrin IX (PpIX) as natural photosensitizer derived from administration of 5-aminolevulinic acid (5-ALA) has found clinical use for photodiagnosis and photodynamic therapy of several cancers. However, broader use of 5-ALA in oncology is hampered by its charge and polarity that result in its reduced capacity for passing biological barriers and reaching the tumor tissue. Advanced drug delivery platforms are needed to improve the biodistribution of 5-ALA. Here, we report a new approach for the delivery of 5-ALA. Squalenylation strategy was used to covalently conjugate 5-ALA to squalene, a natural precursor of cholesterol. 5-ALA-SQ nanoassemblies were formed by self-assembly in water. The nanoassemblies were monodisperse with average size of 70 nm, polydispersity index of 0.12, and ζ -potential of +36 mV. They showed good stability over several weeks. The drug loading of 5-ALA was very high at 26 %. In human prostate cancer cells PC3 and human glioblastoma cells U87MG PpIX production was monitored *in vitro* upon the incubation with nanoassemblies. The results showed that they were highly efficient in generating PpIX-induced fluorescence in cancer cells and demonstrate a novel nano-delivery platform for the systemic administration of 5-ALA.

Keywords: 5-aminolevulinic acid, nanoassemblies, fluorescence, photodetection, photodynamic therapy

Background

Medical nanotechnology has introduced promising new drug delivery platforms. They are composed from biocompatible and biodegradable nanomaterials that help to improve chemical stability and pharmacokinetic profile of pharmacologically active compounds, while providing a controlled delivery at the site of action.¹ However, only few nanoparticle systems have so far reached the market. The main pitfalls of existing nanoparticles (NPs) are mainly their poor drug loading (usually less than 5 %) and “burst release effect” which brings about a premature release of significant portion of the drug before reaching the target site. This causes adverse side effects, and might lead to toxicity, and loss of pharmacological activity.²

*Correspondence: Andrej Babič, Rue Michel Servet 1, 1211 Geneva, Switzerland, +41 22 379 36 78, andrej.babic@unige.ch

Squalene (SQ) is a linear triterpene with the chemical formula $C_{30}H_{50}$ and a precursor of cholesterol and other steroids.³ In the human body, squalene is synthesized in the liver and in the skin and transported by low density lipoprotein (LDL) and very low density lipoprotein (VLDL) in the blood.⁴ In the context of tumor therapy squalene exhibited a strong potentiation effect on certain chemotherapeutic agents.⁵ Because it is widely found in nature and safe, squalene has found its applications in pharmaceutical technology as an excipient in the preparation of lipid emulsions for the delivery of vaccines, various active compounds and genes.^{4,6} Squalene has been found suitable for the covalent conjugation to different drugs. Advanced nanosystems created this way incorporate squalene conjugated to chemotherapeutic agents like gemcitabine,⁷ paclitaxel,⁸ cisplatin,⁹ or doxorubicin.¹⁰ This approach is called “squalenoylation” and involves prodrug strategy with the formation of the nano-colloidal systems where the active principle is covalently bound.¹¹ Squalene based nanoassemblies (NAs) are formed by self-assembly of functional components in aqueous media and are characterized by inherent high drug loading.¹² Squalenoylation has been found to enhance drug stability, increase the solubility of poorly water-soluble drugs hence improving bioavailability and prolonging drug half-life in the systemic circulation.^{9,11a} In most cases, such self-assembled NAs display better pharmacological activity than the parent drug.^{11a,13} In addition, squalenoylation provides a mean to construct NAs containing both a therapeutic and an imaging modality.¹⁴ Similar theranostic NAs have been reported by Couvreur and co-workers by incorporating a MRI agent into squalenoyl-gemcitabine (SQgem) nanoassemblies.⁹ These types of multifunctional systems may be of a major importance in developing new theranostic agents for personalized medicine.

In the context of cancer theranostics, the administration of a small molecule 5-aminolevulinic acid (5-ALA) (**Figure 1**) has led to the clinical use of 5-ALA for photodynamic therapy (PDT),¹⁵ photodiagnosis (PD)¹⁶ and fluorescence-guided tumor resection in brain cancer glioma patients.¹⁷ The theranostics is achieved by the metabolism of 5-ALA and selective accumulation of protoporphyrin IX (PpIX) within the cancer tissue as a consequence of the bypassed feedback inhibition of the heme cycle.¹⁸ However, the efficacy of 5-ALA PD and PDT is seriously hampered by its zwitterionic nature at neutral pH found in the bloodstream. Different attempts have been made to improve 5-ALA's stability and pharmacokinetic profile. Both the amino- and the carboxylic- end of 5-ALA have been modified by various approaches.¹⁹ The esterification of 5-ALA's carboxyl group has led to 5-ALA methyl ester (Metvix®)²⁰ is used in the topical treatment of actinic keratosis, basal cell carcinoma, and acute acne. Hexyl ester of 5-ALA (5-ALA-Hex) (Hexvix®) has gained marketing authorization for the photodiagnosis (PD) of bladder cancer²¹ and is experimentally exploited for the treatment of cervical cancer and severe acne.²²

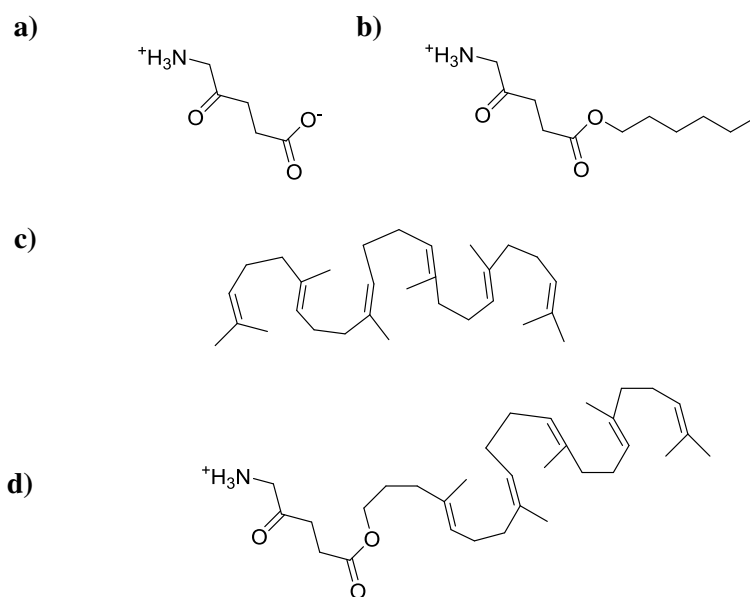


Fig 1. Chemical structures of NA building block elements. 5-ALA (a), 5-ALA-Hex (b), squalene (c) and 5-ALA-SQ (d).

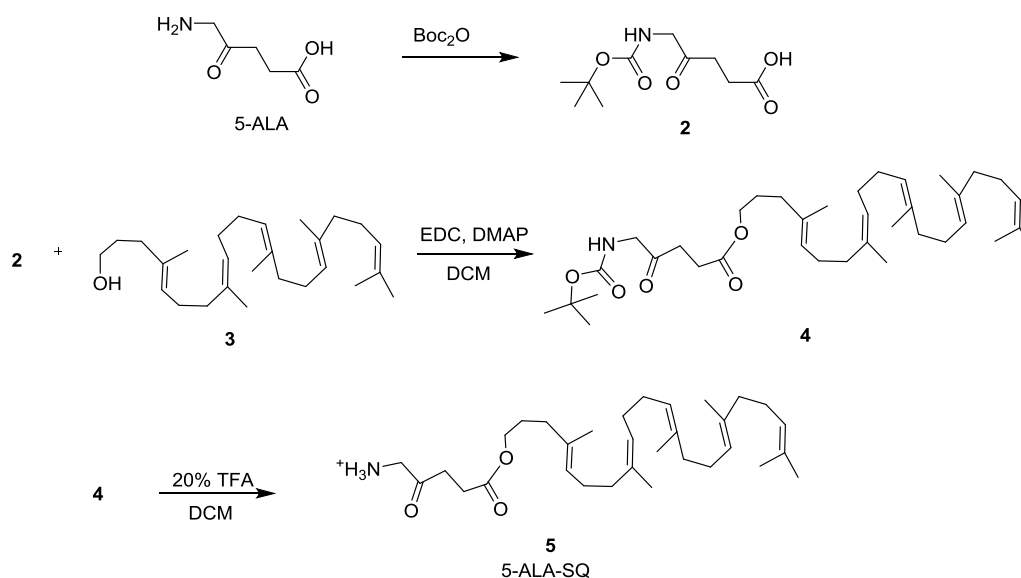
However, with the exception of GliolanTM the clinical use of 5-ALA and its derivatives is mostly limited to topical administration. This limits their use in more important types of cancer, such as breast, colorectal, lung and prostate cancer. Attempts to broaden the use of 5-ALA has amino-end modified phosphatase-sensitive derivatives of 5-ALA that have shown very promising activity recently.²³ Furthermore, attempts have been undertaken to encapsulate 5-ALA into different nano systems including polymeric NAs²⁴ or liposomes²⁵ and its conjugation into dendrimers²⁶, or gold NPs.²⁷ Although some of these solutions have helped to improve 5-ALA stability and its pharmacokinetic profile, none of aforementioned attempts have resulted in a successful clinical candidate in the field of cancer nanomedicine.

The aim of this work was the design and synthesis of 5-ALA-squalene (5-ALA-SQ) conjugate building block (**Figure 1d**) that self-assembles in aqueous media and contains high drug loading of 5-ALA, a prerequisite for pharmacological activity in cancers. The NAs were tested on two different cancer cell lines for their fluorescence PD capabilities. Combined with recent reports of squalene based NAs exploiting plasma lipoproteins to achieve indirect cancer targeting,²⁸ this 5-ALA nanotechnology approach expand the use of 5-ALA for PD and PDT of different cancers, such as prostate cancer used in this study.

Results and Discussion

5-ALA-SQ building block synthesis

An efficient converging chemical strategy was used to synthesize the 5-ALA-SQ building block from squalene and 5-ALA (**Scheme 1**). 5-ALA was first protected at the amino end with *N*-Boc protecting group using standard conditions. Nanoassembly-inducing squalene alcohol (**3**) was synthesized from squalene in 4 synthetic steps according to procedures described in the literature.²⁹ Boc-5-ALA (**2**) and squalene alcohol were then coupled in the presence of EDC and DMAP to yield the protected ester derivative (**4**) in good yield. The final Boc deprotection had to be performed under mild acidic conditions to avoid electrophilic addition onto the squalene scaffold. The final product was purified by reverse-phase HPLC to yield the NA building block in good yield.



Scheme 1. 5-ALA-SQ building block synthesis.

5-ALA-SQ nanoassemblies

In order to achieve an efficient delivery of an active compound by nanoparticles (NPs) to its site of action, parameters such as nanoparticle size, shape and surface charge play an important role and govern the pharmacokinetics of nano-delivery systems in the body.³⁰ In particular, particle size governs several pharmacokinetic phenomena such as NP half-life in the systemic circulation, sequestration by macrophages and the extravasation through leaky vasculature into the site of action³¹. Shape and size of nanoparticles regulate their ability to extravasate through the fenestrations found in the vasculature³⁰⁻³¹. Size and shape are also very important for active targeting and uptake into cells since smaller NP

and spherical shapes have a smaller surface area thus much limited contact points in comparison to larger non-spherical nanoparticulate systems.³¹

The self-assembly of 5-ALA-SQ building block occurred spontaneously in aqueous media. The NAs were formed by nanoprecipitation. 5-ALA-SQ conjugate was dissolved in organic solvents and was added dropwise into water. Total evaporation of the organic solvents yielded an aqueous solution of NAs. 5-ALA-SQ NAs were monodisperse with low polydispersity index of 0.12. Electrophoretic mobility measurements gave ζ -potential of 36 mV and dynamic light scattering (DLS) revealed monodisperse distribution of NAs with an average size of 70 nm (**Figure 2**). The NA size range offers good potential for prolonged circulation in the bloodstream.³⁰ Nevertheless, 5-ALA-SQ NAs are significantly smaller than previously reported SQ composites which ranges between 100-300 nm indicating a different supramolecular arrangement.¹³

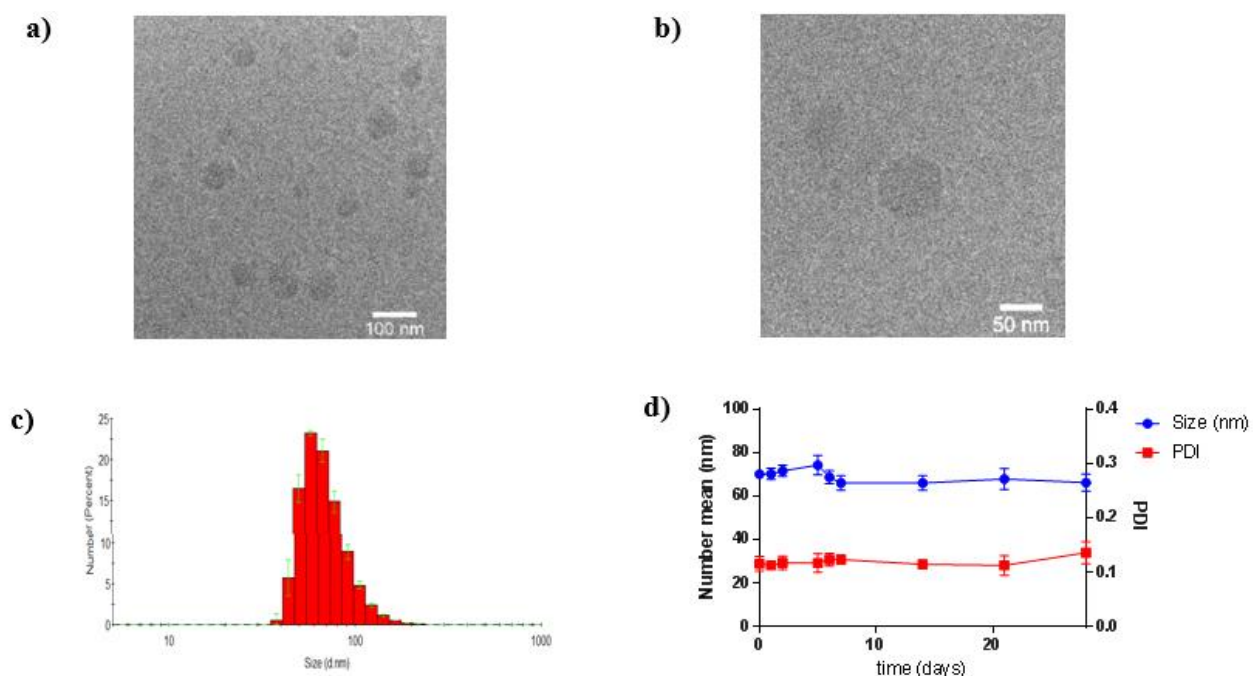


Fig 2. Characterization of ALA-SQ NAs. Low (a) and high (b) magnification cryo-TEM images, DLS analysis (c), and stability at 4 °C (d).

The smaller size might be due to positively charged amino-groups and relatively small 5-ALA molecule in comparison to SQ moiety. It has been demonstrated that the variation of small molecules attached to squalene, introduces changes in self-assembly and packing of compound-squalene conjugates consequently altering the shape and size of NAs.^{11a} It is possible that the highly positively charged amino group of 5-ALA orients itself toward the bulk water whilst the lipophilic chains occupy the interior of these NAs, however the exact supramolecular structure remains to be elucidated. Despite

the significantly smaller size compared to other squalene nanocomposites the NAs display excellent shelf stability with size and PDI remaining constant over several weeks.

Another important aspect of the new 5-ALA-SQ NAs is that they achieve a drug loading of 26 % which is high in comparison to other reported 5-ALA nanoparticulate systems where the loading was much less efficient.^{24a, 24b, 25b} Drug loading is very important in NP delivery because in poor drug loaded NPs, administered dose might not be sufficient for reaching pharmacologically active concentration in target tissues.² The loading could be determined by simple calculation taking into account the molecular weights of 5-ALA and 5-ALA-SQ since 5-ALA is covalently bound to the squalene scaffold in 1:1 molar ratio.

PpIX fluorescence kinetic measurements in cancer cells

Time-dependent formation of PpIX was evaluated in PC3 human prostate cancer cells and U87MG glioblastoma incubated with 5-ALA-SQ NAs and 5-ALA-Hex as reference. **Figure 3** presents the PpIX formation in PC3 human prostate cancer cells exposed to increasing concentrations of 5-ALA-SQ NAs or 5-ALA-Hex over 24 h.

Concentration-dependent PpIX fluorescence profiles were observed for 5-ALA-SQ NAs. At 1.0 and 2.0 mM PpIX fluorescence increased steadily over 24 h, whilst reaching a plateau after 8 h of incubation for lower concentrations. On the other hand, 5-ALA-Hex induced the highest accumulation of PpIX in lower concentration range between 0.10 and 0.30 mM as reported previously.^{23a, 32} However, 5-ALA-Hex at concentrations above 1 mM was found to be toxic to cells which reduces the overall fluorescence observed and impedes its use.^{23b}

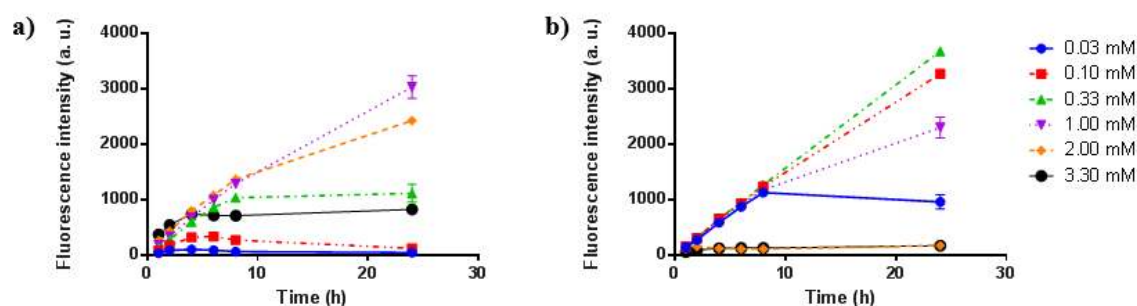


Fig 3. Kinetic fluorescence measurements of PpIX accumulation in PC3 cells. The cells were incubated with increasing concentrations of 5-ALA-SQ NAs (a) or 5-ALA-Hex (b).

Next, dose-dependent PpIX accumulation in PC3 and U87MG human glioblastoma cancer cells was performed with the goal of estimating optimal NA dosing. Fluorescence intensity at 4 h and 24 h of incubation with 5-ALA-SQ NAs and 5-ALA-Hex is shown in **Figure 4**. Very importantly, 5-ALA-SQ NAs induced the PpIX production in both cell lines. Furthermore, maximum fluorescence levels are comparable with ALA-Hex control in both cell lines. It can also be noted that in PC3 cells, 1.0 and 2.0 mM concentrations of 5-ALA-SQ NAs were optimal for inducing the highest accumulation of PpIX.

In U87MG cells, there was no significant differences between different concentrations of 5-ALA-SQ NAs for short incubation times (**Figure 4c**). At 24 h, PpIX accumulation was found to be dependent on the concentration of 5-ALA-SQ NAs or 5-ALA-Hex similar to PC3 cells. A decrease in PpIX induction somewhat similar to ALA-Hex was found after longer period of incubation at higher concentrations of 5-ALA-SQ NAs which were more sensitive to the presence of NAs.

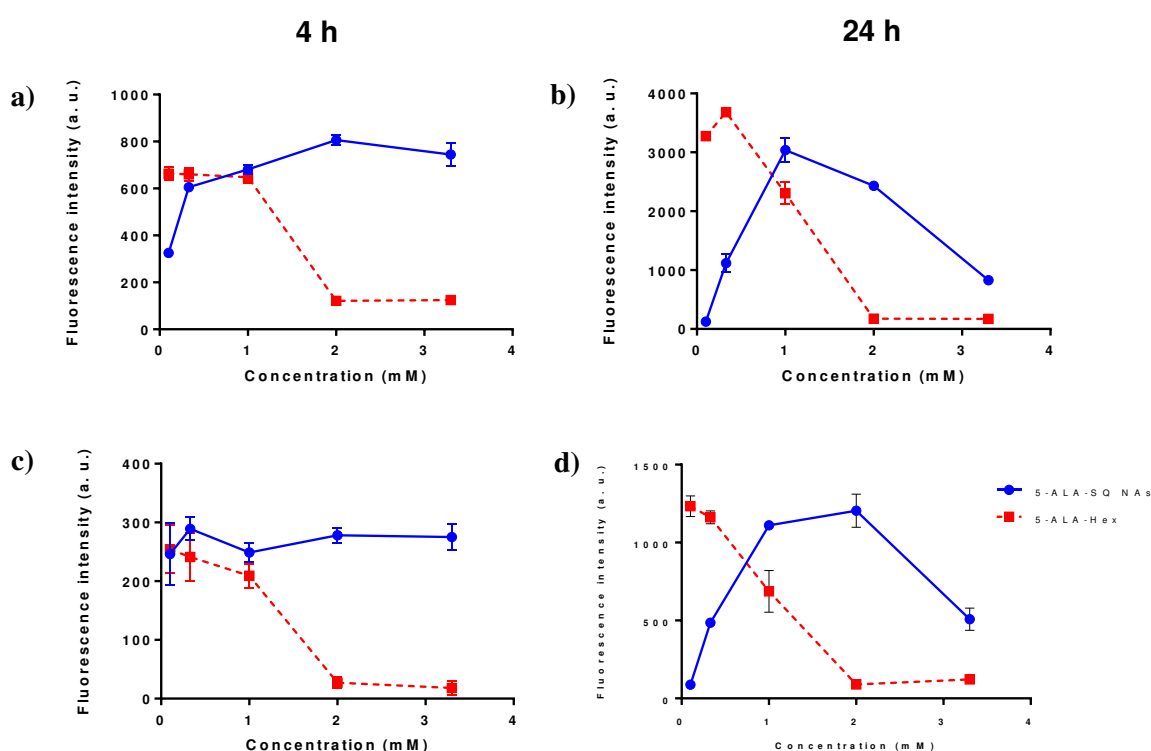


Fig 4. Dose-response curves. Concentration-dependent PpIX accumulation with 5-ALA-SQ NAs (blue) and 5-ALA-Hex (red) in PC3 (a, b) and U87MG (c, d) cells after 4 h (left) and 24 h (right) incubation

Figure 4 demonstrates that at 24 h PpIX production curves are bell-shaped in both PC3 and U87MG cells. Whilst 1 mM concentration of 5-ALA-SQ NAs induced the highest PpIX accumulation in PC3 cells, U87MG cells tolerated higher concentrations and the increase in PpIX fluorescence was seen up to 2 mM 5-ALA-SQ NAs. In general, higher concentrations of 5-ALA-SQ NAs were needed to efficiently induce the biosynthesis of PpIX when compared to 5-ALA-Hex, presumably due to the different ester bond cleavage rates within the cancer cells. Decrease in PpIX production was observed when concentrations higher than 1 mM of 5-ALA-Hex used due to the non-specific toxicity of 5-ALA-Hex. However, the fluorescence levels were similar for both compounds without any fluorescence lag observed for the NAs.

The NAs were also assayed in U87MG glioblastoma against 5-ALA control which is marketed for PD of glioblastoma during surgical resection. **Figure 5** presents the fluorescence of U87MG cell after 4 h and 24 h. 5-ALA-SQ NAs induced significantly higher fluorescence after 4 h compared to 5-ALA which is highly-relevant in a clinical setting. At 24 h the fluorescence profile shifts in favor of 5-ALA at lower concentrations as the slow, active uptake of 5-ALA affords sufficient 5-ALA quantities within the cells. NAs still demonstrate similar fluorescence levels to 5-ALA at optimal 1.0 and 2.0 mM concentrations of NAs (**Figure 5b**).

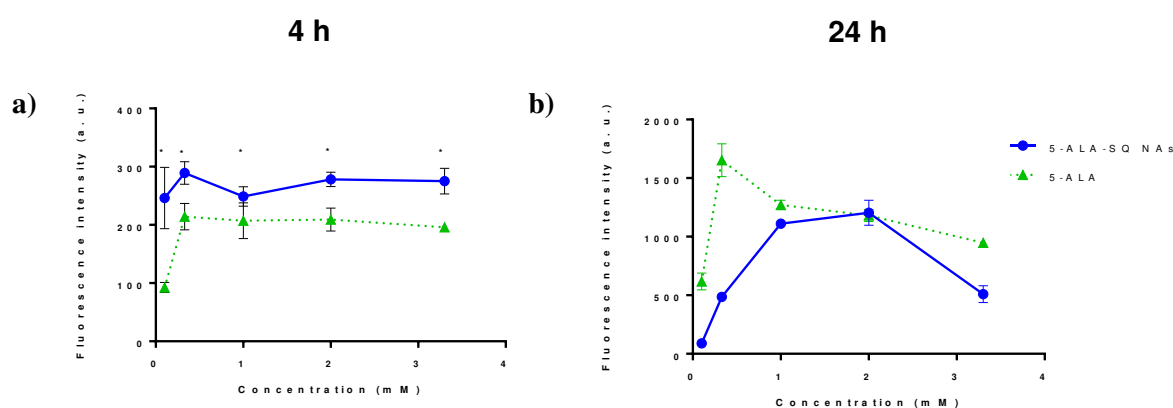


Fig 5. Dose-response curves. Concentration-dependent PpIX accumulation in U87MG cells after 4 h (a) and 24 h (b) incubation with 5-ALA-SQ NAs (blue) and 5-ALA (green).

In clinical practice, 5-ALA is administered either topically or orally but, because of its charged nature, only small portion of the initial dose enters into target cells via endogenous peptide transporters like PEPT1, PEPT2 or BETA transporters, depending on the cell type.^{25a, 33} Recent studies on NAs from a SQgem derivative indicate that the cell entry is governed by albumin-enhanced diffusion of single molecule building blocks and it was found to be highly dependent on presence of extracellular proteins.³⁴ Furthermore, far-red fluorescent NAs we reported recently also demonstrated rapid internalization³⁵ and 5-ALA-SQ fluorescence kinetic experiments and the dose-response curves corroborate single molecule building block internalization of and efficient subsequent metabolism to yield fluorescent PpIX.

Conclusions

In this *in vitro* proof-of-concept study, a converging chemical strategy was used to synthesize the 5-ALA-SQ building block from squalene and 5-ALA. The 5-ALA-SQ NAs were prepared by spontaneous nanoprecipitation in water. NAs were monodisperse and stable with size average of 70 nm, polydispersity index of 0.12, positive ζ -potential of 36 mV and high, 26 % 5-ALA loading. PpIX production was evaluated *in vitro* in two cancer cell lines by measuring the fluorescence increase over time and compared to 5-ALA and 5-ALA-Hex. The results showed that SQ-ALA NAs are very efficient in inducing the PpIX production in PC3 and U87MG cancer cell types. In scope with these findings, we can conclude that 5-ALA-SQ NAs present an attractive nanotechnology solution for overcoming the pharmacokinetic drawbacks of 5-ALA. Further *in vivo* experiments will evaluate their potential for the systemic delivery of 5-ALA for fluorescence PD and PDT therapy of tumors.

Experimental

Reagents were purchased from commercial suppliers Sigma-Aldrich (Bucks, Switzerland) and Acros Organics (Basel, Switzerland) and used without further purification. Deuterated NMR solvents were obtained from Cambridge Isotope Laboratories (Tewksbury, USA). Tetrahydrofuran (THF) and dichloromethane (CH₂Cl₂) were obtained from an Anhydrous Engineering alumina column based drying system. All other solvents used were HPLC grade. N,N-dimethylformamide (DMF), methanol (CH₃OH), diethyl ether (Et₂O) and acetone were purchased from Sigma-Aldrich (Buchs, Switzerland). Ethyl acetate (AcOEt) was purchased from Biosolve (Dieuze, France), acetonitrile (CH₃CN) was supplied by Carlo Erba Reagents (Balerna, Switzerland). Hexane \geq 95 % of n-hexane was purchased from Fisher Chemical (Basel, Switzerland). The water used for the preparations was deionized by a

Milli-Q lab water system (Millipore, Molsheim, France). Chemical reactions were performed using standard syringe-septa with positive pressure of argon to ensure anhydrous conditions.

Thin layer chromatography (TLC) was performed with aluminium backed silica plates (Merck-Keisegel 60 F254) with a suitable mobile phase and was visualized using a UV fluorescence lamp (254 and 366 nm) and/or developed with ninhydrine, 20 % sulfuric acid or phosphomolybdic acid (PMA). Flash chromatography was performed on an automated PuriFlash® 4100 machine from Interchim (Montlucon, France) using Interchim silica columns puriFlash® HP 30 µm equipped with a PDA detector (200 – 800 nm) and automated fraction collector. The elution profile was monitored using Flash Interchim software version 5.0x. Semi-preparative HPLC column was conducted on a Waters Symmetry 300TM - 5 µm (19 x 150 mm), C8 column (Baden-Dättwil, Switzerland). Analytical UPLC was conducted using Macherey-Nagel EC50/2 Nucleodur Gravity 1.8 µm column (50 x 2.1 mm) fitted on a Waters system equipped with a Waters PDA detector (Baden-Dättwil, Switzerland). Buffer A = CH₃CN + 0.1 % Formic acid), buffer B = H₂O + 0.1 % Formic acid. Flow rate = 400.0 µL/min at 25 °C. ¹H and ¹³C NMR spectra were recorded on Varian Gemini 300 MHz, Varian Innova 500 MHz or Bruker Avance III Cryo 600 MHz spectrometers at 298 K. Chemical shifts (δ) are quoted in parts per million (ppm) and coupling constants (J) are in hertz (Hz). s for singlet, d for doublet, dd for doublet of doublets, t for triplet, q for quartet, m for multiplet. Residual solvent peaks were used as the internal reference for the proton and carbon chemical shifts. NMR spectra were processed with Mnova version 10.0.2 software package. Low resolution mass spectrometry (LRMS) was carried out on a HTS PAL-LC10A – API 150Ex instrument in ESI (positive mode). High resolution mass spectrometry (HRMS) was carried out on a QSTAR Pulsar (AB/MDS Sciex) instrument in ESI (positive mode). Chemical structures were drawn and named according IUPAC nomenclature using ChemBioDraw Ultra version 14.0.0.117 software package. The pH was measured on a Metrohm 691 pH meter using a spearhead electrode (Zofingue, Switzerland), calibrated with Metrohm buffers. Statistical analyses were performed using GraphPad Prism 6, 2016, (GraphPad Software) software. P-value < 0.05 was considered as statistically significant.

Synthesis of SQ-ALA building block

5-(tert-Butoxycarbonylamino)-4-oxopentanoic Acid (2)

Boc-5-ALA was synthesized according to published procedure. The spectroscopic data are identical with the literature.³⁶ ¹H NMR (600 MHz, DMSO-d₆) δ 12.12 (s, 1H), 7.06 (t, J = 5.9 Hz, 1H), 3.76 (d, J = 5.9 Hz, 2H), 2.61 (t, J = 6.6 Hz, 2H), 2.40 (t, J = 6.5 Hz, 2H), 1.38 (s, 9H). ¹³C NMR (151 MHz, DMSO) δ 206.62, 174.07, 156.21, 78.54, 49.97, 40.38, 40.24, 40.11, 39.97, 39.83, 39.69, 39.55, 34.22, 28.64. [M+H]⁺ 232.1, found 232.7.

(4E,8E,12E,16E)-4,8,13,17,21-pentamethyldocosa-4,8,12,16,20-pentaen-1-ol (3)

Squalene alcohol **3** was synthesized from squalene in 4 synthetic steps in 23.7% yield as colourless oil according to the reported procedures.²⁹ ¹H NMR (300 MHz, CDCl₃) δ 5.17-5.06 (m, 5H, CH), 3.62 (q, *J* = 6.3 Hz, 2H, CH₂-OH), 2.17 – 1.92 (m, 18H, CH₂), 1.67 (s, 3H, CH₃), 1.59 (m, 17 H, CH₃ and CH₂). ¹³C NMR (75 MHz, CDCl₃) δ 135.35, 135.17, 135.14, 134.81, 131.49, 125.05, 124.64, 124.60, 124.47, 63.07, 39.98, 39.95, 39.89, 36.24, 30.92, 28.48, 26.98, 26.88, 26.78, 25.94, 17.92, 16.28, 16.23, 16.08. LRMS (ESI): *m/z* calculated for [M+NH₄]⁺ 404.4, found 404.8.

(4E,8E,12E,16E)-4,8,13,17,21-pentamethyldocosa-4,8,12,16,20-pentaen-1-yl 5-((tert-butoxy carbonyl)amino)-4-oxopentanoate (4)

Squalene alcohol (**3**) (100 mg, 0.26 mmol), EDC (74 mg, 0.38 mmol) and DMAP (94 mg, 0.78 mmol), and 5-(tert-Butoxycarbonylamino)-4-oxopentanoic acid (**2**) (77 mg, 0.34 mmol) were dissolved in DCM (15 mL). After stirring overnight at ambient temperature the solvent was evaporated under reduced pressure and crude product purified by Flash chromatography using DCM/ethyl acetate (EA) gradient giving colorless oil (108 mg, 0.18 mmol, 70 %). ¹H NMR (300 MHz, CDCl₃) δ 5.31 – 5.20 (br s, 1H), 5.13 – 5.07 (m, 5H), 4.09 – 3.95 (m, 4H), 2.75 – 2.53 (m, 4H), 2.02 – 1.95 (m, 20H), 1.64 (s, 3H), 1.63 – 1.50 (m, 19H), 1.41 (s, 9H). ¹³C NMR (75 MHz, CDCl₃) δ 204.46, 172.65, 135.30, 135.16, 135.09, 133.75, 131.43, 125.34, 124.60, 124.57, 124.48, 124.45, 64.81, 50.53, 39.96, 39.93, 39.87, 35.92, 34.56, 28.52, 28.47, 28.43, 28.24, 28.02, 26.97, 26.86, 25.92, 23.11, 17.90, 16.25, 16.21, 16.06. LRMS (ESI): *m/z* calculated for [M+NH₄]⁺ 617.5, found 617.8.

Trifluoroacetic acid salt of 5-amino-(((4E,8E,12E,16E)-4,8,13,17,21-pentamethyldocosa-4,8,12,16,20-pentaen-1-yl)oxy)-4-oxopentanoate (5)

Compound **4** (34 mg, 57 μmol) was dissolved in DCM (2.0 mL). Trifluoroacetic acid (TFA) (200 μL) was added and the reaction mixture stirred at ambient temperature. After 10 min the solvents were evaporated in vacuo at low temperature and traces of TFA were removed by co-evaporation with EA (3x10 mL). The crude product was purified by RP-HPLC using full H₂O/AcN (0.025 % TFA) gradient yielding colorless oil (25 mg, 74 %). ¹H NMR (300 MHz, CDCl₃) δ 5.31 – 5.20 (br s, 1H), 5.13 – 5.07 (m, 5H), 4.09 – 3.95 (m, 4H), 2.75 – 2.53 (m, 4H), 2.02 – 1.95 (m, 20H), 1.64 (s, 3H), 1.63 – 1.50 (m, 19H). LRMS (ESI): *m/z* calculated for [M+H]⁺ 500.4, found 500.6.

Preparation of nanoassemblies.

NAs were prepared by nanoprecipitation described in detail elsewhere.³⁷ Briefly, building block **5** (1.2 mg, 2.0 μmol) was dissolved in a 50/50 V/V mixture acetone/ethanol (500 μL). The organic phase was then added dropwise using a micro-syringe into MilliQ water (1.25 mL) at 100 $\mu\text{L}/\text{min}$ under magnetic stirring. After 5 min under stirring the magnetic stir bar was removed and the organic solvents and the excess of water removed using a rotary evaporator at 30 $^{\circ}\text{C}$. The final concentration of nanoassemblies was 2.00 mM.

Characterization of 5-ALA-SQ NAs

5-ALA loading of 5-ALA.SQ NA was calculated from the respective contributions of the molecular weights of 5-ALA and of 5-ALA-SQ conjugate as follows:¹³

$$\text{Loading (\%)} = \frac{MW(5 - ALA)}{MW(5 - ALA - SQ)} \times 100$$

Hydrodynamic diameter of NAs was measured by dynamic light scattering (DLS) using a NANO ZS instrument from Malvern (Worcestershire, UK) running the ZetaSizer 7.01 software. The analyses were performed with 4 mW He-Ne Laser (633 nm) at scattering angle of 173 $^{\circ}$ at 25 $^{\circ}\text{C}$ in Polystyrene (PS) micro cuvette from Brand (Wertheim, Germany). Zeta potential (ZP) was determined using the same Nano ZS instrument from Malvern in folded capillary cells DTS 1070 from Malvern. Size distribution and size mean diameter were calculated from the data. The stability of NAs stored at 4 $^{\circ}\text{C}$ was assayed by DLS at regular time points over a period of 1 month.

The morphology of NAs was assessed by cryogenic transmission electron microscope (cryo-TEM) using TECNAI[®] G² Sphera microscope (FEI, Thermo Fisher Scientific) equipped with 2000 by 2000 pixel high resolution digital camera TCL (Gräfelfing, Germany). The vitrified-ice samples were prepared using the Virtobot cryo-plunger (FEI, Thermo Fisher Scientific). NAs (2.0 μL , 2.0 mM) were applied to Quantifoil Cu/Rh 200 mesh R3.5/1 grids (SPI, West Chester, USA) and vitrified using liquid ethane.

Cell culture

Human prostate cancer cells PC3 (ATTC[®] CRL-1435TM) and human glioblastoma cells U87MG (ATTC[®] HTB-14TM) were grown and maintained by serial passage in F-12K nutrient mix (21127-022, Thermo Fisher Scientific) or minimum Essential Media (31095-029, Thermo Fisher Scientific), respectively. Cell media were supplemented with fetal calf serum (10 %, CVFVSF00-01, Eurobio), streptomycin (100 $\mu\text{L}/\text{mL}$) and penicillin (100 IU/mL, 15140-122, Thermo Fisher Scientific). Cells were cultivated at 37 $^{\circ}\text{C}$ in a humidified atmosphere containing 95 % air and 5 % CO_2 .

In vitro PpIX fluorescence kinetic measurements

Human prostate cancer cells PC3 (12,000 cells/well) and glioblastoma cells U87MG (10,000 cells/well) were seeded in 96-well plates (clear bottom black plate, 3603, Corning). The next day, cells were exposed to increasing concentrations of 5-ALA-SQ NAs, 5-ALA-Hex, and 5-ALA in U87MG cells. PpIX fluorescence was recorded with a plate reader (Safire, Tecan, Switzerland) at different time points. Excitation wavelength was set to 405 nm and emission wavelength to 630 nm. Mean values and s.d. for each concentration at each time point per plate were subtracted with the reference value (no treatment) and plotted for each cell line.

Declarations

Acknowledgements

We thank Dr. Christoph Bauer and Jérôme Bosset from the Bioimaging platform at the University of Geneva for their input and help with cryo-TEM experiments. We are grateful to Dr. Laurence Marcourt of the School of Pharmaceutical Sciences Geneva-Lausanne for her contribution in NMR experiments. We would also like to acknowledge the Mass Spectrometry platform at the University of Geneva for the mass spectroscopy analysis. We thank Canton of Geneva, Switzerland and Swiss National Science Foundation for funding. This work was supported, by grants from the Swiss National Science Foundation (205321_173027).

Authors' Contributions

AB and NL conceived and designed the whole study. AB, VH, EB carried out the experiments and analyzed the data. AB wrote the manuscript. HPL, LB and NL provided helpful suggestions. All authors read and approved the final manuscript.

Competing Interests

The authors declare that they have no competing interests.

Publisher's Note

Springer Nature remains neutral with regard to jurisdictional claims in published maps and institutional affiliations.

Author details

¹ School of Pharmaceutical Sciences, University of Geneva, University of Lausanne, Rue Michel Servet 1, 1211 Geneva 4, Switzerland

² Centre de Recherche en Automatique de Nancy (CRAN), CNRS UMR 7039 (Centre National de la Recherche Scientifique), Université de Lorraine, Campus Sciences, Vandœuvre-lès-Nancy, France

³ Institut de Cancérologie de Lorraine, Research Department, Avenue de Bourgogne, 54519 Vandœuvre-lès-Nancy, France

References

1. (a) Torchilin, V. P. Multifunctional nanocarriers. *Adv Drug Deliv Rev* **2006**, *58* (14), 1532-55; (b) Zhang, L.; Gu, F. X.; Chan, J. M.; Wang, A. Z.; Langer, R. S.; Farokhzad, O. C. Nanoparticles in medicine: therapeutic applications and developments. *Clin Pharmacol Ther* **2008**, *83* (5), 761-9; (c) Fishman, W. H.; Anlyan, A. J. The presence of high beta-glucuronidase activity in cancer tissue. *J Biol Chem* **1947**, *169* (2), 449.
2. Couvreur, P. Nanoparticles in drug delivery: past, present and future. *Adv Drug Deliv Rev* **2013**, *65* (1), 21-3.
3. Acimovic, J.; Rozman, D. Steroidal triterpenes of cholesterol synthesis. *Molecules* **2013**, *18* (4), 4002-17.
4. Reddy, L. H.; Couvreur, P. Squalene: A natural triterpene for use in disease management and therapy. *Advanced drug delivery reviews* **2009**, *61* (15), 1412-26.
5. Nakagawa, M.; Yamaguchi, T.; Fukawa, H.; Ogata, J.; Komiyama, S.; Akiyama, S.; Kuwano, M. Potentiation by squalene of the cytotoxicity of anticancer agents against cultured mammalian cells and murine tumor. *Jpn J Cancer Res* **1985**, *76* (4), 315-20.
6. (a) Huang, Z. R.; Lin, Y. K.; Fang, J. Y. Biological and Pharmacological Activities of Squalene and Related Compounds: Potential Uses in Cosmetic Dermatology. *Molecules* **2009**, *14* (1), 540-554; (b) Fox, C. B. Squalene emulsions for parenteral vaccine and drug delivery. *Molecules* **2009**, *14* (9), 3286-312.
7. (a) Reddy, L. H.; Dubernet, C.; Mouelhi, S. L.; Marque, P. E.; Desmaele, D.; Couvreur, P. A new nanomedicine of gemcitabine displays enhanced anticancer activity in sensitive and resistant leukemia types. *J Control Release* **2007**, *124* (1-2), 20-7; (b) Reddy, L. H.; Ferreira, H.; Dubernet, C.; Mouelhi, S. L.; Desmaele, D.; Rousseau, B.; Couvreur, P. Squalenoyl nanomedicine of gemcitabine is more potent after oral administration in leukemia-bearing rats: study of mechanisms. *Anticancer Drugs* **2008**, *19* (10), 999-1006; (c) Reddy, L. H.; Marque, P. E.; Dubernet, C.; Mouelhi, S. L.; Desmaele, D.; Couvreur, P. Preclinical toxicology (subacute and acute) and efficacy of a new squalenoyl gemcitabine anticancer nanomedicine. *J Pharmacol Exp Ther* **2008**, *325* (2), 484-90.
8. Dosio, F.; Reddy, L. H.; Ferrero, A.; Stella, B.; Cattel, L.; Couvreur, P. Novel nanoassemblies composed of squalenoyl-paclitaxel derivatives: synthesis, characterization, and biological evaluation. *Bioconjugate chemistry* **2010**, *21* (7), 1349-61.
9. Arias, J. L.; Reddy, L. H.; Othman, M.; Gillet, B.; Desmaele, D.; Zouhiri, F.; Dosio, F.; Gref, R.; Couvreur, P. Squalene Based Nanocomposites: A New Platform for the Design of Multifunctional Pharmaceutical Theragnostics. *Acs Nano* **2011**, *5* (2), 1513-1521.
10. Maksimenko, A.; Dosio, F.; Mouglin, J.; Ferrero, A.; Wack, S.; Reddy, L. H.; Weyn, A. A.; Lepeltier, E.; Bourgaux, C.; Stella, B.; Cattel, L.; Couvreur, P. A unique squalenoylated and nonpegylated doxorubicin nanomedicine with systemic long-circulating properties and anticancer activity. *Proceedings of the National Academy of Sciences of the United States of America* **2014**, *111* (2), E217-26.
11. (a) Lepeltier, E.; Bourgaux, C.; Rosilio, V.; Poupaert, J. H.; Meneau, F.; Zouhiri, F.; Lepetre-Mouelhi, S.; Desmaele, D.; Couvreur, P. Self-assembly of squalene-based nucleolipids: relating the chemical structure of the bioconjugates to the architecture of the nanoparticles. *Langmuir : the ACS journal of surfaces and colloids* **2013**, *29* (48), 14795-803; (b) Couvreur, P.; Stella, B.; Reddy, L. H.; Hillaireau, H.; Dubernet, C.; Desmaele, D.; Lepetre-Mouelhi, S.; Rocco, F.; Dereuddre-Bosquet, N.; Clayette, P.; Rosilio, V.; Marsaud, V.; Renoir, J. M.; Cattel, L. Squalenoyl nanomedicines as potential therapeutics. *Nano Lett* **2006**, *6* (11), 2544-8.
12. Bui, D. T.; Nicolas, J.; Maksimenko, A.; Desmaele, D.; Couvreur, P. Multifunctional squalene-based prodrug nanoparticles for targeted cancer therapy. *Chemical communications* **2014**, *50* (40), 5336-8.
13. Desmaele, D.; Gref, R.; Couvreur, P. Squalenoylation: a generic platform for nanoparticulate drug delivery. *Journal of controlled release : official journal of the Controlled Release Society* **2012**, *161* (2), 609-18.

14. Babič, A.; Pascal, S.; Duwald, R.; Moreau, D.; Lacour, J.; Allémann, E. [4]Helicene–Squalene Fluorescent Nanoassemblies for Specific Targeting of Mitochondria in Live-Cell Imaging. *Adv Funct Mater*, 1701839-n/a.
15. (a) Peng, Q.; Warloe, T.; Berg, K.; Moan, J.; Kongshaug, M.; Giercksky, K. E.; Nesland, J. M. 5-Aminolevulinic acid-based photodynamic therapy. Clinical research and future challenges. *Cancer* **1997**, *79* (12), 2282-308; (b) Dirschka, T.; Radny, P.; Dominicus, R.; Mensing, H.; Bruning, H.; Jenne, L.; Karl, L.; Sebastian, M.; Oster-Schmidt, C.; Klovekorn, W.; Reinhold, U.; Tanner, M.; Grone, D.; Deichmann, M.; Simon, M.; Hubinger, F.; Hofbauer, G.; Krahn-Senftleben, G.; Borrosch, F.; Reich, K.; Berking, C.; Wolf, P.; Lehmann, P.; Moers-Carpi, M.; Honigsmann, H.; Wernicke-Panten, K.; Helwig, C.; Foguet, M.; Schmitz, B.; Lubbert, H.; Szeimies, R. M.; Group, A.-C. S. Photodynamic therapy with BF-200 ALA for the treatment of actinic keratosis: results of a multicentre, randomized, observer-blind phase III study in comparison with a registered methyl-5-aminolaevulinate cream and placebo. *Br J Dermatol* **2012**, *166* (1), 137-46.
16. Inada, N. M.; Costa, M. M.; Guimaraes, O. C.; Ribeiro Eda, S.; Kurachi, C.; Quintana, S. M.; Lombardi, W.; Bagnato, V. S. Photodiagnosis and treatment of condyloma acuminatum using 5-aminolevulinic acid and homemade devices. *Photodiagnosis Photodyn Ther* **2012**, *9* (1), 60-8.
17. (a) Stummer, W.; Pichlmeier, U.; Meinel, T.; Wiestler, O. D.; Zanella, F.; Reulen, H. J.; Group, A. L.-G. S. Fluorescence-guided surgery with 5-aminolevulinic acid for resection of malignant glioma: a randomised controlled multicentre phase III trial. *The Lancet. Oncology* **2006**, *7* (5), 392-401; (b) Tonn, J. C.; Stummer, W. Fluorescence-guided resection of malignant gliomas using 5-aminolevulinic acid: practical use, risks, and pitfalls. *Clinical neurosurgery* **2008**, *55*, 20-6; (c) Hefti, M.; Mehdorn, H. M.; Albert, I.; Dorner, L. Fluorescence-Guided Surgery for Malignant Glioma: A Review on Aminolevulinic Acid Induced Protoporphyrin IX Photodynamic Diagnostic in Brain Tumors. *Curr Med Imaging Rev* **2010**, *6* (4), 254-258.
18. Peng, Q.; Warloe, T.; Berg, K.; Moan, J.; Kongshaug, M.; Giercksky, K. E.; Nesland, J. M. 5-aminolevulinic acid-based photodynamic therapy - Clinical research and future challenges. *Cancer* **1997**, *79* (12), 2282-2308.
19. Fotinos, N.; Campo, M. A.; Popowycz, F.; Gurny, R.; Lange, N. 5-Aminolevulinic acid derivatives in photomedicine: Characteristics, application and perspectives. *Photochemistry and photobiology* **2006**, *82* (4), 994-1015.
20. Foley, P. Clinical efficacy of methyl aminolevulinate (Metvix) photodynamic therapy. *J Dermatolog Treat* **2003**, *14 Suppl 3*, 15-22.
21. (a) Lange, N.; Jichlinski, P.; Zellweger, M.; Forrer, M.; Marti, A.; Guillou, L.; Kucera, P.; Wagnieres, G.; van den Bergh, H. Photodetection of early human bladder cancer based on the fluorescence of 5-aminolaevulinic acid hexylester-induced protoporphyrin IX: a pilot study. *Br J Cancer* **1999**, *80* (1-2), 185-93; (b) Lapini, A.; Minervini, A.; Masala, A.; Schips, L.; Pycha, A.; Cindolo, L.; Giannella, R.; Martini, T.; Vittori, G.; Zani, D.; Bellomo, F.; Cosciani Cunico, S. A comparison of hexaminolevulinate (Hexvix((R))) fluorescence cystoscopy and white-light cystoscopy for detection of bladder cancer: results of the HeRo observational study. *Surg Endosc* **2012**, *26* (12), 3634-41.
22. (a) Andrejevic-Blant, S.; Major, A.; Ludicke, F.; Ballini, J. P.; Wagnieres, G.; van den Bergh, H.; Pelte, M. F. Time-dependent hexaminolaevulinate induced protoporphyrin IX distribution after topical application in patients with cervical intraepithelial neoplasia: A fluorescence microscopy study. *Lasers Surg Med* **2004**, *35* (4), 276-83; (b) Hillemanns, P.; Wang, X.; Hertel, H.; Andikyan, V.; Hillemanns, M.; Stepp, H.; Soergel, P. Pharmacokinetics and selectivity of porphyrin synthesis after topical application of hexaminolevulinate in patients with cervical intraepithelial neoplasia. *Am J Obstet Gynecol* **2008**, *198* (3), 300 e1-7; (c) Soergel, P.; Makowski, L.; Makowski, E.; Schippert, C.; Hertel, H.; Hillemanns, P. Treatment of high grade cervical intraepithelial neoplasia by photodynamic therapy using hexylaminolevulinate may be costeffective compared to conisation procedures due to decreased pregnancy-related morbidity. *Lasers Surg Med* **2011**, *43* (7), 713-20.
23. (a) Babic, A.; Herceg, V.; Ateb, I.; Allemann, E.; Lange, N. Tunable phosphatase-sensitive stable prodrugs of 5-aminolevulinic acid for tumor fluorescence photodetection. *J Control Release* **2016**, *235*, 155-64; (b) Herceg, V.; Lange, N.; Allemann, E.; Babic, A. Activity of phosphatase-

sensitive 5-aminolevulinic acid prodrugs in cancer cell lines. *Journal of photochemistry and photobiology. B, Biology* **2017**, *171*, 34-42.

24. (a) Chung, C. W.; Chung, K. D.; Jeong, Y. I.; Kang, D. H. 5-aminolevulinic acid-incorporated nanoparticles of methoxy poly(ethylene glycol)-chitosan copolymer for photodynamic therapy. *International journal of nanomedicine* **2013**, *8*, 809-19; (b) Shi, L.; Wang, X.; Zhao, F.; Luan, H.; Tu, Q.; Huang, Z.; Wang, H.; Wang, H. In vitro evaluation of 5-aminolevulinic acid (ALA) loaded PLGA nanoparticles. *International journal of nanomedicine* **2013**, *8*, 2669-76; (c) Wang, X. J.; Shi, L.; Tu, Q. F.; Wang, H. W.; Zhang, H. Y.; Wang, P. R.; Zhang, L. L.; Huang, Z.; Zhao, F.; Luan, H. S.; Wang, X. L. Treating cutaneous squamous cell carcinoma using 5-aminolevulinic acid poly(lactic-co-glycolic acid) nanoparticle-mediated photodynamic therapy in a mouse model. *International journal of nanomedicine* **2015**, *10*, 347-355.
25. (a) Plaunt, A. J.; Harmatys, K. M.; Hendrie, K. A.; Musso, A. J.; Smith, B. D. Chemically triggered release of 5-aminolevulinic acid from liposomes. *RSC Adv* **2014**, *4* (101), 57983-57990; (b) Di Venosa, G.; Hermida, L.; Batlle, A.; Fukuda, H.; Defain, M. V.; Mamone, L.; Rodriguez, L.; MacRobert, A.; Casas, A. Characterisation of liposomes containing aminolevulinic acid and derived esters. *Journal of photochemistry and photobiology. B, Biology* **2008**, *92* (1), 1-9; (c) Pierre, M. B.; Tedesco, A. C.; Marchetti, J. M.; Bentley, M. V. Stratum corneum lipids liposomes for the topical delivery of 5-aminolevulinic acid in photodynamic therapy of skin cancer: preparation and in vitro permeation study. *BMC Dermatol* **2001**, *1*, 5; (d) Kosobe, T.; Moriyama, E.; Tokuoka, Y.; Kawashima, N. Size and surface charge effect of 5-aminolevulinic acid-containing liposomes on photodynamic therapy for cultivated cancer cells. *Drug Dev Ind Pharm* **2005**, *31* (7), 623-9.
26. (a) Battah, S. H.; Chee, C. E.; Nakanishi, H.; Gerscher, S.; MacRobert, A. J.; Edwards, C. Synthesis and biological studies of 5-aminolevulinic acid-containing dendrimers for photodynamic therapy. *Bioconjugate chemistry* **2001**, *12* (6), 980-8; (b) Casas, A.; Battah, S.; Di Venosa, G.; Dobbin, P.; Rodriguez, L.; Fukuda, H.; Batlle, A.; MacRobert, A. J. Sustained and efficient porphyrin generation in vivo using dendrimer conjugates of 5-ALA for photodynamic therapy. *Journal of controlled release : official journal of the Controlled Release Society* **2009**, *135* (2), 136-43.
27. (a) Oo, M. K.; Yang, X.; Du, H.; Wang, H. 5-aminolevulinic acid-conjugated gold nanoparticles for photodynamic therapy of cancer. *Nanomedicine* **2008**, *3* (6), 777-86; (b) Zhang, Z.; Wang, S.; Xu, H.; Wang, B.; Yao, C. Role of 5-aminolevulinic acid-conjugated gold nanoparticles for photodynamic therapy of cancer. *Journal of biomedical optics* **2015**, *20* (5), 51043.
28. Sobot, D.; Mura, S.; Yesylevskyy, S. O.; Dalbin, L.; Cayre, F.; Bort, G.; Mouglin, J.; Desmaele, D.; Lepetre-Mouelhi, S.; Pieters, G.; Andreiuk, B.; Klymchenko, A. S.; Paul, J. L.; Ramseyer, C.; Couvreur, P. Conjugation of squalene to gemcitabine as unique approach exploiting endogenous lipoproteins for drug delivery. *Nat Commun* **2017**, *8*, 15678.
29. Ceruti, M.; Balliano, G.; Rocco, F.; Lenhart, A.; Schulz, G. E.; Castelli, F.; Milla, P. Synthesis and biological activity of new iodoacetamide derivatives on mutants of squalene-hopene cyclase. *Lipids* **2005**, *40* (7), 729-35.
30. Longmire, M.; Choyke, P. L.; Kobayashi, H. Clearance properties of nano-sized particles and molecules as imaging agents: considerations and caveats. *Nanomedicine* **2008**, *3* (5), 703-17.
31. Blanco, E.; Shen, H.; Ferrari, M. Principles of nanoparticle design for overcoming biological barriers to drug delivery. *Nat Biotechnol* **2015**, *33* (9), 941-51.
32. Casas, A.; Perotti, C.; Saccoliti, M.; Sacca, P.; Fukuda, H.; Batlle, A. M. ALA and ALA hexyl ester in free and liposomal formulations for the photosensitisation of tumour organ cultures. *Br J Cancer* **2002**, *86* (5), 837-42.
33. Rodriguez, L.; Batlle, A.; Di Venosa, G.; Battah, S.; Dobbin, P.; MacRobert, A. J.; Casas, A. Mechanisms of 5-aminolevulinic acid ester uptake in mammalian cells. *British journal of pharmacology* **2006**, *147* (7), 825-33.
34. (a) Bildstein, L.; Marsaud, V.; Chacun, H.; Lepetre-Mouelhi, S.; Desmaele, D.; Couvreur, P.; Dubernet, C. Extracellular-protein-enhanced cellular uptake of squalenoyl gemcitabine from nanoassemblies. *Soft Matter* **2010**, *6* (21), 5570-5580; (b) Bildstein, L.; Dubernet, C.; Marsaud, V.; Chacun, H.; Nicolas, V.; Gueutin, C.; Sarasin, A.; Benech, H.; Lepetre-Mouelhi, S.; Desmaele, D.; Couvreur, P. Transmembrane diffusion of gemcitabine by a nanoparticulate squalenoyl prodrug: An original drug delivery pathway. *Journal of Controlled Release* **2010**, *147* (2), 163-170.

35. Babic, A.; Pascal, S.; Duwald, R.; Moreau, D.; Lacour, J.; Allemann, E. [4] Helicene-Squalene Fluorescent Nanoassemblies for Specific Targeting of Mitochondria in Live-Cell Imaging. *Adv Funct Mater* **2017**, *27* (33).
36. Berkovitch, G.; Doron, D.; Nudelman, A.; Malik, Z.; Rephaeli, A. Novel Multifunctional Acyloxyalkyl Ester Prodrugs of 5-Aminolevulinic Acid Display Improved Anticancer Activity Independent and Dependent on Photoactivation. *J Med Chem* **2008**, *51* (23), 7356-7369.
37. Maksimenko, A.; Dosio, F.; Mouglin, J.; Ferrero, A.; Wack, S.; Reddy, L. H.; Weyn, A. A.; Lepeltier, E.; Bourgaux, C.; Stella, B.; Cattel, L.; Couvreur, P. A unique squalenoylated and nonpegylated doxorubicin nanomedicine with systemic long-circulating properties and anticancer activity. *Proceedings of the National Academy of Sciences of the United States of America* **2014**, *111* (2), E217-E226.